Am J Transl Res 2022;14(5):3344-3359
www.ajtr.org /ISSN:1943-8141/AJTR0141966

Original Article

Hemodynamic analysis of intermittent pneumatic compression combined with hyperthermia after total hip arthroplasty: an experiment on male rabbits

Siping Zhang[1*], Pengcheng Ma[1*], Aikeremujiang Muheremu[2*], Rongxin Sun[3], Hao Chai[1], Kan Jiang[1]

[1]Department of Orthopedics, Sixth Affiliated Hospital of Xinjiang Medical University, Urumqi 830002, Xinjiang, P. R. China; [2]Department of Spine Surgery, Sixth Affiliated Hospital of Xinjiang Medical University, Urumqi 830002, Xinjiang, P. R. China; [3]Department of Orthopedics, Chengdu Second People's Hospital, Chengdu 610000, Sichuan, P. R. China. [*]Equal contributors and co-first authors.

Received January 23, 2022; Accepted April 28, 2022; Epub May 15, 2022; Published May 30, 2022

Abstract: Objective: To investigate the effect of intermittent pneumatic compression combined with hyperthermia (IPCH) on the hemodynamic changes in lower limbs of male rabbits and to clarify whether its efficacy is superior to that of intermittent pneumatic compression (IPC) or hyperthermia (HT) alone. Methods: Thirty male adult New Zealand white rabbits with a body mass of 2.6±0.3 kg were obtained to establish a model of postoperative hypercoagulable state by simulating left hip surgery. Then they were randomly divided into HT group, IPC group, and IPCH group. Relevant hemodynamic parameters were examined by color Doppler ultrasound before and after treatment. A femoral vein finite element model was established according to fluid mechanics to analyze the blood flow velocity distribution vector, total deformation, equivalent stress of the femoral vein and venous valve. Results: The heart rate, blood flow per minute, and mean and peak blood velocity of the femoral vein in IPCH group were significantly higher than those in HT and IPC groups ($P<0.05$). There was no significant difference in venous diameter ($P>0.05$). The blood flow velocity distribution vector, the total deformation of femoral vein, and the equivalent stress between femoral vein and venous valve in the IPCH group were higher than those in HT and IPC groups, but the total deformation of venous valve was smaller in IPCH group. Conclusions: IPCH superimposes the effects of IPC and HT, and can more effectively promote changes in local blood circulation to prevent deep vein thrombosis.

Keywords: Deep vein thrombosis, physical prophylaxis, intermittent pneumatic compression, hyperthermia, hemodynamics

Introduction

As an effective treatment for diseases such as end-stage osteoarthritis, ischemic necrosis of femoral head, and femoral neck fractures in elderly patients, total hip arthroplasty (THA) can significantly improve quality of life [1-3]. Deep vein thrombosis (DVT) in the lower limbs is one of the most common complications after THA [4-6]. DVT not only severely compromises the patient's postoperative recovery, but also may lead to life-threatening pulmonary embolism [7, 8]. Prophylactic measures for DVT mainly include basic prophylaxis, physical prophylaxis, and pharmacologic prophylaxis [9]. Intermittent pneumatic compression (IPC) is one of the common physical prophylactic measures used in clinical practice [10, 11]. The combination of IPC and pharmacologic prophylaxis can achieve better effects [12]. An increase in local blood flow is the most important physiologic effect of hyperthermia (HT) [13, 14]. The blood flow rate of leg muscles is closely related to local tissue temperature, and thermal stimulation can effectively increase the blood circulation of muscles and promote deep venous return [15-18]. The local blood perfusion volume increases approximately 15 times when the local temperature reaches 41°C-45°C [19]. Shujiro et al. [20] found effective improvement of hemodynamics and vascular endothelial function after applying 45°C heating to the calf for 20 min. Both IPC and thermal stimulation can change the hemodynamics of lower limbs. However, whether the combined effect of IPC and HT is superior to the effect of IPC or HT

Figure 1. Experimental facilities. A. Intermittent pneumatic compression device; B. Homemade hyperthermia device.

alone has not been investigated. In this paper, we obtained the hemodynamic parameters after simulating hip surgery in male rabbits, and preliminarily explored the efficacy of intermittent pneumatic compression combined with hyperthermia (IPCH) by finite element hemodynamic analysis.

Materials and methods

Research subjects

Thirty healthy male New Zealand white rabbits, with a body mass of 2.6±0.3 Kg were purchased from the Animal Experiment Center of Xinjiang Medical University. License number: SCXK (Xin) 2018-0002. Each rabbit was raised in a single cage. The indoor circadian rhythm was kept for 12 hours, the room temperature was kept at 22-24°C, and the humidity was kept at 50%-60%. The rabbits were fed once a day in the morning or evening and they drank water freely.

Experimental methods

Simulated hip surgery: The blood hypercoagulable state model was established after simulated hip surgery in 30 male rabbits. The anesthetic was Zoletil®50 (VIRBAC France Co. LTD) and Xylazine Hydrochloride Injection (Dunhua Shengda Animal Medicine Co. LTD) mixture in a 1:1 proportion, and rabbits were anesthetized by intramuscular injection (0.1 ml/Kg). After successful anesthesia and disinfection, a 3 cm long left lateral thigh incision was made to separate the skin and subcutaneous tissue layer by layer, and fully expose the femur. A hole was drilled and a metal screw was placed in the proximal left femur, and then the incision was washed and sutured by layers. The lower limbs were fixed in a hip cast after the simulated surgery.

Interventions: Thirty rabbits were divided into the HT group, IPC group, and IPCH group according to a random number table, with 10 rabbits in each group. The researcher completed the experiment in a quiet environment on the first day after simulated surgery. The hemodynamics of the left lower limbs were measured after rabbits were anesthetized, and then the treatment regimens were completed: (1) HT group: the heating soft board was wrapped and secured around the lower limbs. Considering that a high temperature may damage the thin skin of rabbits, we set the temperature at 40°C. The duration was set as 20 min; (2) IPC group: the intermittent pneumatic compression device (IPCD) was used (the chambers were inflated in turn and deflated at the same time after all of them were filled with pressure). The pressure was usually set between 40 and 60 mmHg [11], and the most commonly used pressure on the thigh was 60 mmHg [21, 22]. To better simulate the effect of “muscle pump”, the treatment pressure was set at 60 mmHg, and the treatment time was set as 20 min; (3) IPCH group: the whole lower limb was wrapped with the heating soft board, and the temperature was set at 40°C. The pressure leg sheath of the IPCD was wrapped on the outside of the heating soft board. The treatment pressure was 60 mmHg and the treatment time was 20 min. IPC and HT devices are shown in **Figure 1**. For the convenience of description and comparison, physiologic hemodynamic parameters of rabbits were set to the Normal group, and the hemodynamic parameters after simulated left hip surgery (before treatment) were set to the HSS group.

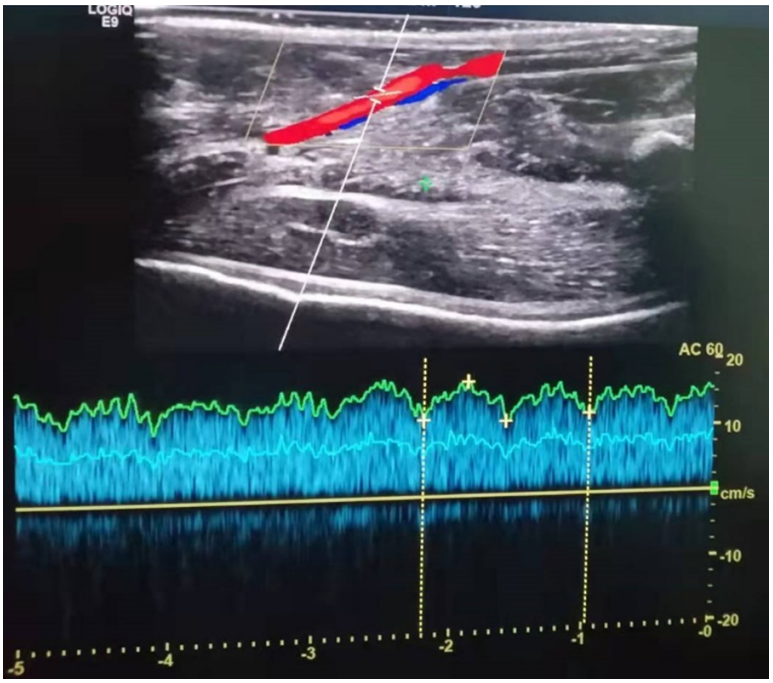

Figure 2. The hemodynamic values are detected by CDFI.

Measurement of hemodynamic parameters: Color Doppler Flow Imaging (CDFI) was used to measure the femoral venous hemodynamic parameters in Normal and HSS groups, and it was measured within 1 min after treatment in HT, IPC and IPCH groups. The hemodynamic parameters detected by CDFI are shown in **Figure 2**. Then we integrated the hemodynamic parameters and calculated the Reynolds number (Re) to determine the blood flow state. Re was calculated by $Re=\rho vd/\mu$, where ρ is the blood density (Kg/m^3), v is the mean blood velocity (m/s), d is the vessel diameter (m), and μ is the hemodynamic viscosity ($Pa.s/m^2$). The hemodynamic parameters of each group are shown in **Table 1**.

Computed tomography perfusion imaging (CTPI) of femoral vein: A rabbit was randomly selected, anesthetized, and then fixed on a scanning bed in the supine position with lower limbs straight. Then 4.5 mL Iohexol Injection (Yangzijiang Pharmaceutical Group Co. LTD) was injected with a high-pressure syringe at a rate of 1.5 mL/s through the indwelling needle in the marginal ear vein, with a concentration of 300 mg/mL. After that, 10 mL normal saline was injected at the same rate. CTPI (SOMATOM Definition Flash) was performed two times since the beginning of Iohexol injection, and the femoral venous imaging was obtained.

Establishment of femoral venous model: Femoral venous computed tomography (CT) data were processed by Mimics21.0 software, and the venous segment where the great saphenous vein converged on femoral vein (saphenous-femoral junction) was selected and exported as *.STL file through regional growth, threshold segmentation and other functions. The femoral vein was optimized with reverse-engineering software Geomagic Studio 2014 to construct a vessel wall with a thickness of 24 μm [23], and then a geometric model of the vessel wall and blood was obtained. According to the position of the venous valve (proximal to the femoral vein, above the saphen-femoral junction), a venous valve with a thickness of 20 μm was constructed [24, 25]. Unigraphics NX 6.0 software was used to cut and assemble the geometric model of the vessel wall, venous valve and blood to obtain a complete femoral venous model, as shown in **Figure 3**. The long axis and short axis of the femoral vein were 2 mm and 1.6 mm, respectively, detected by ultrasound. The maximum opening degree of the venous valve was usually 60%-70% [26], and therefore the opening degree of the venous valve was set at 60% in our study. The femoral venous hemodynamics were analyzed with the fluid dynamics method by ANSYS Workbench.

Governing equations: Although blood in veins is not pulsating like in arteries, it still has an unsteady flow due to the periodic opening and closing of the venous valve. In order to better simulate the relationship among blood flow, femoral vein and venous valve, we used the fluid-structure interaction model. Blood was treated as an incompressible Newtonian fluid in this study and satisfied the following governing equations:

Continuity equation:

$$\iint_A \bar{n} \cdot \bar{v}\, dA = 0 \quad (1)$$

Where $\bar{n}$ is the normal vector of plane A, and $\bar{v}$ is the velocity vector.

Table 1. Femoral venous hemodynamic parameters (n=10)

Hemodynamic value	Normal	HSS	HT	IPC	IPCH
Mean blood velocity (cm/s)	7.85±0.22	3.58±0.26	5.48±0.50	6.63±0.43	7.05±0.29
Peak blood velocity (cm/s)	17.73±0.94	6.63±0.33	10.22±0.80	11.36±0.43	12.13±0.65
Blood flow per minute (ml/min)	11.43±0.97	4.63±0.47	7.91±0.81	8.46±0.41	9.02±0.44
Heart rate (Times/min)	129.8±4.32	128.5±3.02	137.9±6.87	138.3±4.19	146.5±8.87
Vessel diameter (cm)	0.18±0.01	0.18±0.02	0.18±0.01	0.19±0.01	0.19±0.01
Reynolds number (Re)	37.091	16.916	25.893	33.067	35.162
Blood flow state	Laminar flow	Laminar flow	Laminar flow	Laminar flow	Laminar flow

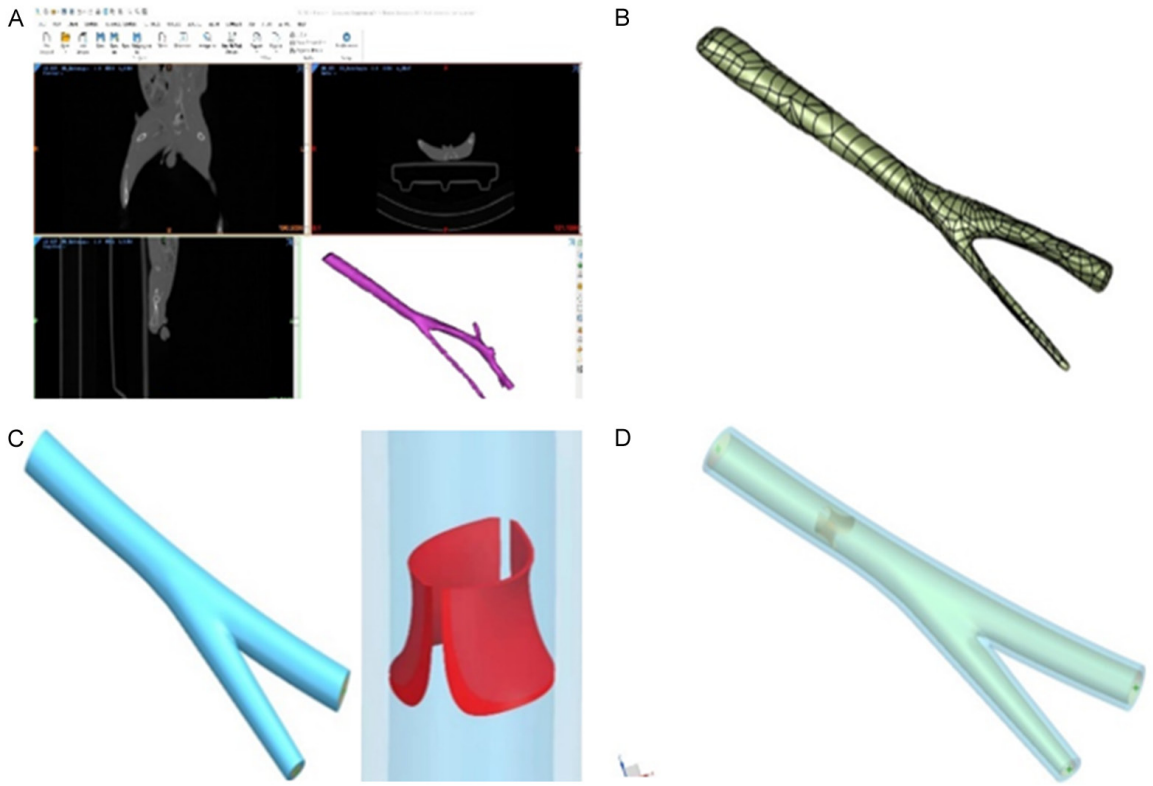

Figure 3. Modeling process of the femoral vein and venous valve. A. CT data are imported and the femoral vein extracted; B. Optimization of grid; C. Establishment of the venous valve model, cutting and assembling of geometric models of the femoral vein and venous valve; D. Complete femoral vein and venous valve model.

Motion equation:

$$\frac{2}{2t}\iiint_{cv}\bar{v}dV+\iint_{cs}\bar{v}_n\bar{v}dA=\iiint_{cv}\bar{f}dV+\iint_{cs}\frac{\bar{p}_n}{\rho}dA \quad (2)$$

Where CV is the control body, CS is the control surface, $\bar{v}_n$ is the surface normal vector component of the velocity, $\bar{f}$ is the external force term (including the stress term), and $\bar{p}_n$ is the surface normal component of the pressure term.

Energy equation:

$$\frac{d}{dt}\iiint_{v}(u+\frac{\bar{v}^2}{2})dV=\frac{2}{2t}\iiint_{cv}(u+\frac{\bar{v}^2}{2})dV+\iint_{cs}\bar{v}_n(u+\frac{\bar{v}^2}{2})dA \quad (3)$$

Where V is the volume of the system, and u is the thermodynamic property.

Dynamic constitutive equation:

$$\mathcal{T}(t)+\frac{\eta\rho}{\kappa\rho}=\eta\rho\gamma(t) \quad (4)$$

Where $\eta\rho$ is the coefficient of viscosity, and $\kappa\rho$ is the elastic coefficient.

State equation:

$$p=\rho RT \quad (5)$$

Where R is the thermodynamic parameter, T is temperature, p is pressure, and ρ is density.

Numerical methods: In this study, we selected the fluid computing module, transient computing module, and system coupling module in ANSYS Workbench 2019. Vessels were regarded as linear elastic materials, and the physical parameters of vessels were set as follows: Young's modulus of the vein was 1 Mpa, Young's modulus of the venous valve was 0.2 Mpa, Poisson's ratio was 0.45, and density was 1150 kg/m^3. Blood was considered an incompressible viscous Newtonian fluid with a hemodynamic viscosity of 0.0035 Pa·s and a density of 1060 kg/m^3 [27]. According to ultrasonic detection and Re calculation, the blood flow state of rabbits in each group was laminar flow. Therefore, the laminar flow model was selected. The bi-directional fluid-structure coupling method was used for numerical simulation, and the interface between blood and vessel wall was set as the fluid-solid coupling interface. The blood and vessel models were meshed separately. Considering the simulation process was transient and coupled, the dynamic mesh method was used to mesh the geometric model. To ensure the calculation accuracy, the model was divided into hexahedral grids, including 209,773 units and 724,175 elements. The distal femoral vein and great saphenous vein were set as the inlet, and the proximal femoral vein was set as the outlet. After the convergence, it was found that the mesh deformation was serious and fluid leakage occurred. These phenomena were considered to be caused by the insufficient thickness of the vein and venous valve. We gradually increased the thickness of the venous wall to 300 μm and increased that of the venous valve to 40 μm. After the second time of convergence, no obvious deformation was found in the mesh, and the convergence accuracy was within the range of 10^{-5}. The time step was set as 0.06 s, and the total duration was set as 3 s.

Initial conditions and boundary conditions: Initial conditions: The femoral venous mean blood velocity in each group was taken (**Table 1**) as the entrance velocity. Since the outlet velocity was basically stable, the outlet pressure was set at 0 Pa [28].

Boundary conditions: The blood, vessel and venous valve were set without slip or permeability boundary.

Outcome indicators

① Blood flow velocity distribution vector of the femoral vein; ② Blood flow state around venous valve; ③ Total deformation of the femoral vein and venous valve; ④ Relationship between the change of total deformation and time; ⑤ Distribution of equivalent stress of femoral vein and venous valve; ⑥ Relationship between the change of equivalent stress and time.

Statistical analysis

SPSS26.0 was used for the analysis of ultrasonic detection results. The normal distribution data were expressed as $\bar{x}\pm S$. The same sample data were tested by paired samples t test under different conditions. The variance analysis was performed for comparison among groups, and the difference was statistically significant if $P<0.05$.

Results

Ultrasonic test results

The mean blood velocity, peak blood velocity, and blood flow per minute in the three groups were significantly increased, and the increase rate in the IPCH group was faster than that in the HT group or IPC group ($P\leq0.001$); The heart rate in the IPCH group was significantly higher than that in the HT group or IPC group ($P<0.05$). However, there was no significant difference in vessel diameter among the three groups ($P>0.05$), as shown in **Table 2**.

Blood flow velocity and state

Blood flow velocity distribution vector of the femoral vein: The middle region of the venous valves showed the most remarkable increase in the femoral vein blood flow velocity, followed by the proximal vein (outlet segment), but the saphenous-femoral junction and the distal vein (inlet segment) had no obvious changes. The blood flow velocity in the HSS group significantly decreased compared with that in the Normal group, but it increased significantly in the three groups. The increased rate of the IPCH group was the most significant, but still lower than that of the Normal group, as shown in **Figure 4**.

Changes of blood flow state around the venous valve: We found that there was a vortex in the

Table 2. Changes n hemodynamic parameters in each group after treatment

Hemodynamic value	HT	IPC	IPCH	*F*	*P*
Mean blood velocity (cm/s)	5.48±0.50	6.63±0.43	7.05±0.29	38.261	<0.001
Peak blood velocity (cm/s)	10.22±0.80	11.36±0.43	12.13±0.65	22.419	<0.001
Blood flow per minute (ml/min)	7.91±0.81	8.46±0.41	9.02±0.44	9.031	0.001
Heart rate (Times/min)	137.9±6.87	138.3±4.19	146.5±8.87	4.925	0.015
Vessel diameter (cm)	0.18±0.01	0.19±0.01	0.19±0.01	0.52	0.6

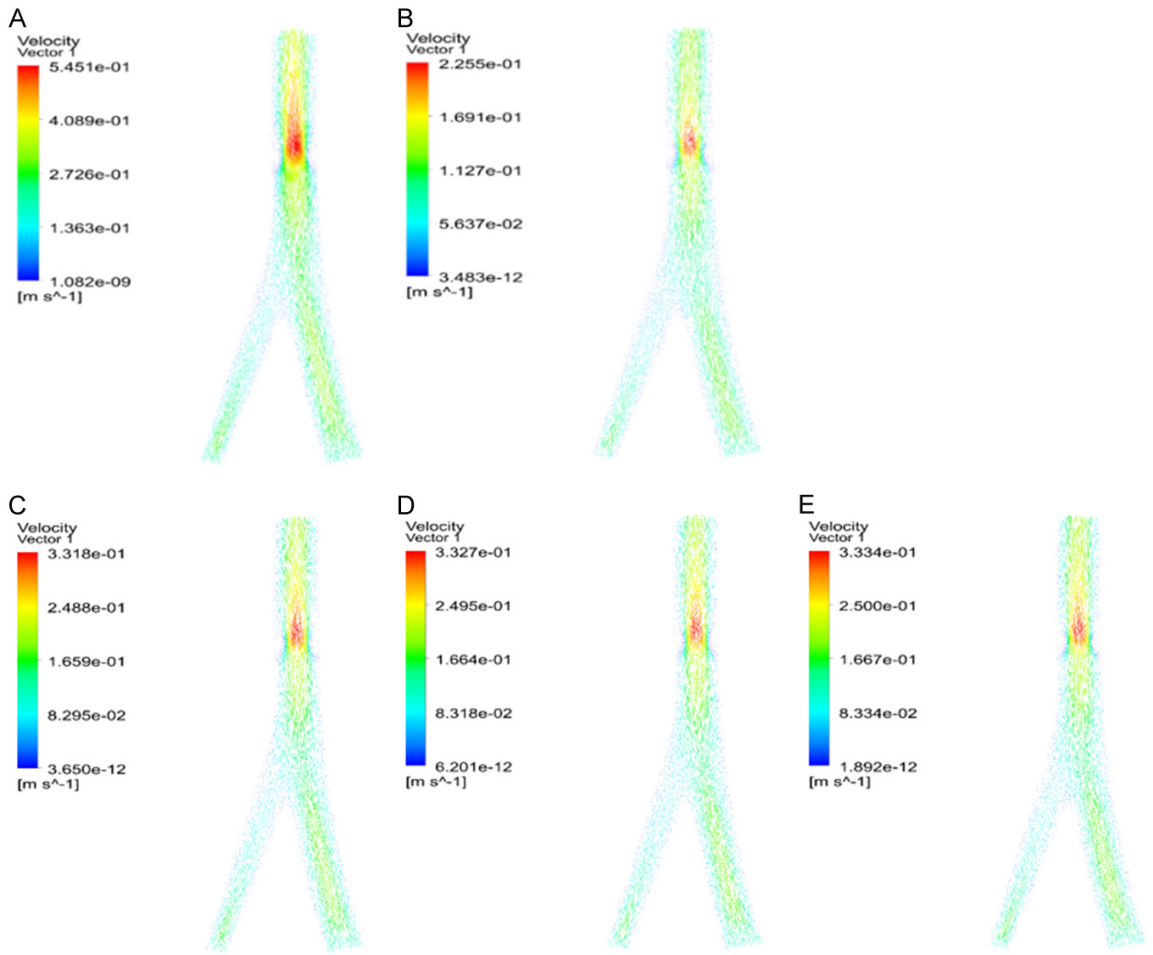

Figure 4. Blood velocity distribution of femoral vein. A. Normal group; B. HSS group; C. HT group; D. IPC group; E. IPCH group.

sinus area around the venous valve, and the flow rate in the vortex was significantly lower than that in other areas of the femoral vein. The blood in the vortex flows into the sinus region first and then returns to the inferior vena cava in the same direction as the main flow. This phenomenon is blood backflow [29]. However, there was no significant difference in the change of the vortex among groups, as shown in **Figure 5**.

Total deformation

Femoral vein: The femoral vein and venous valve were separated and observed. The total deformation of the femoral vein in Normal, HSS and HT groups was significant in the area around the venous valve. The area around the right valve showed the largest deformation, followed by the saphenous-femoral junction. However, the total deformation of saphenous-

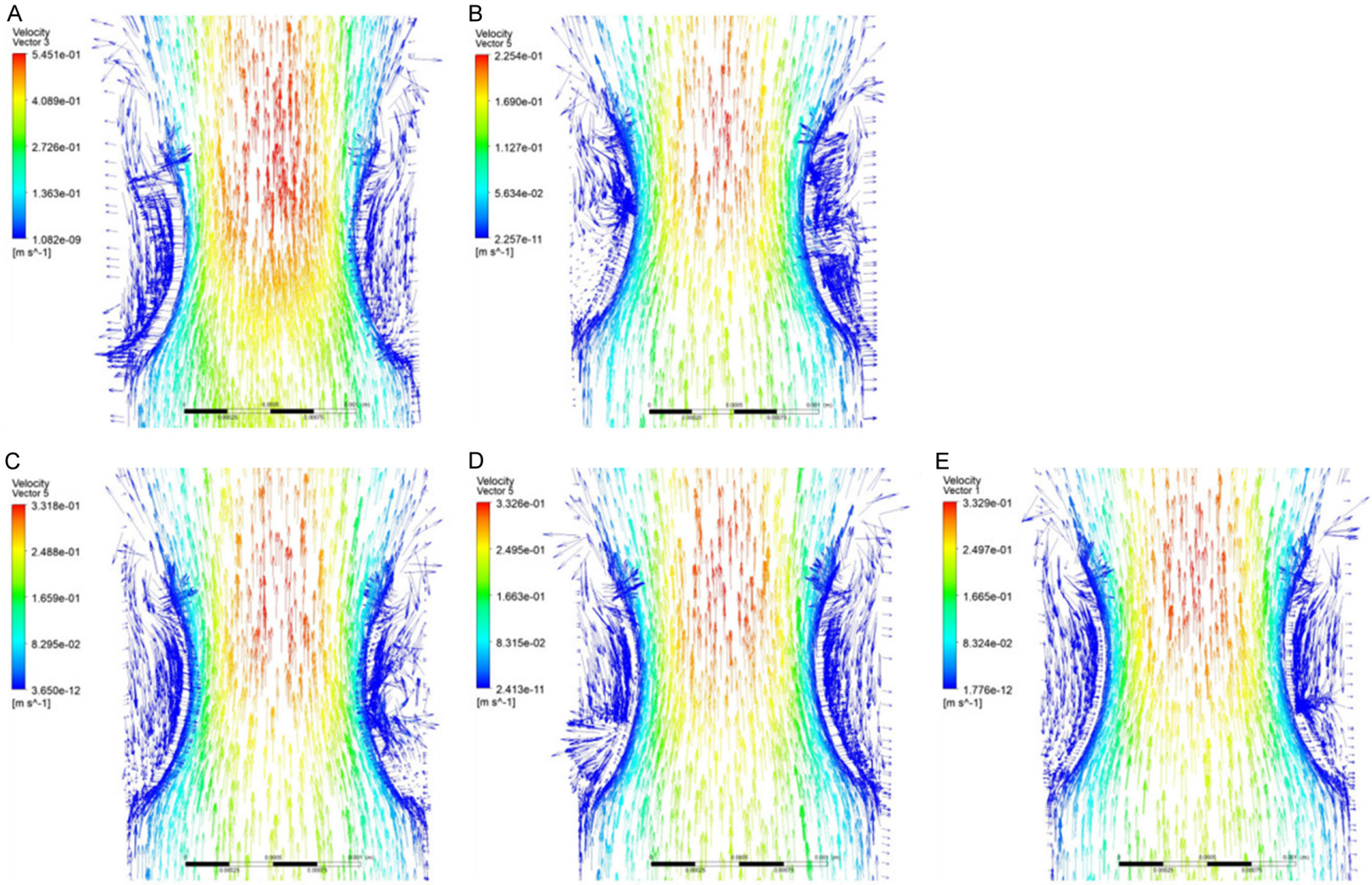

Figure 5. Blood flow state around the venous valve. A. Normal group; B. HSS group; C. HT group; D. IPC group; E. IPCH group.

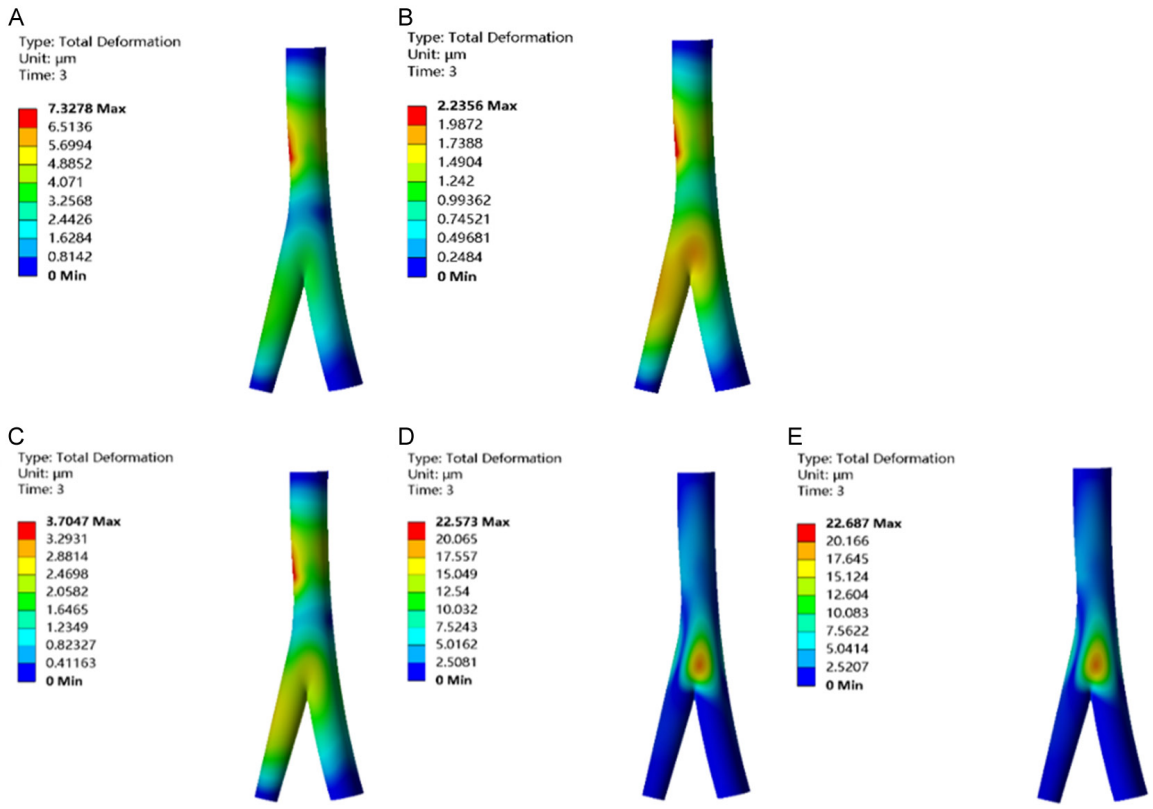

Figure 6. Total deformation of the femoral vein. A. Normal group; B. HSS group; C. HT group; D. IPC group; E. IPCH group.

femoral junction in IPC and IPCH groups was the greatest and higher than that in other parts of the femoral vein due to local compression, as shown in **Figure 6**.

Venous valve: The total deformation was greatest in the upper part of the right venous valve. The total deformation of venous valves in the HSS group significantly decreased compared to that in the Normal group, but the total deformation increased significantly in HT, IPC and IPCH groups compared to that in the HSS group, and the most significant changes were in the HT group, as shown in **Figure 7**.

Relationship between the change of total deformation and time: The relationship between total deformation of the femoral vein and venous valve with time was analyzed after separation, as shown in **Figure 8**. We found that the deformations of the femoral vein and venous valve increased gradually and then decreased with time. The deformation reached a maximum at 1.56 s, and after about 0.4 s, it began to decline in a stepwise fashion. Although the trend of deformation was similar in each group, the amplitude of change was different, and the deformation of the venous valve was larger than that of the femoral vein. The deformation of the femoral vein and venous valve increased significantly after HT, IPC and IPCH, and the changes in IPC and IPCH groups were more significant. The maximum deformation of the IPCH group was larger than that of the IPC group at 1.56 s. The femoral venous deformation in IPC and IPCH groups was slightly larger than that in the Normal group before and after valve opening, but significantly lower than the deformation in the Normal group at the peak stage of valve opening.

Equivalent stress

Femoral vein: The maximal equivalent stress was located in the area around the venous valve in the Normal, HSS, and HT groups. The equivalent stress in the HSS group was lower than that in the Normal group. The equivalent

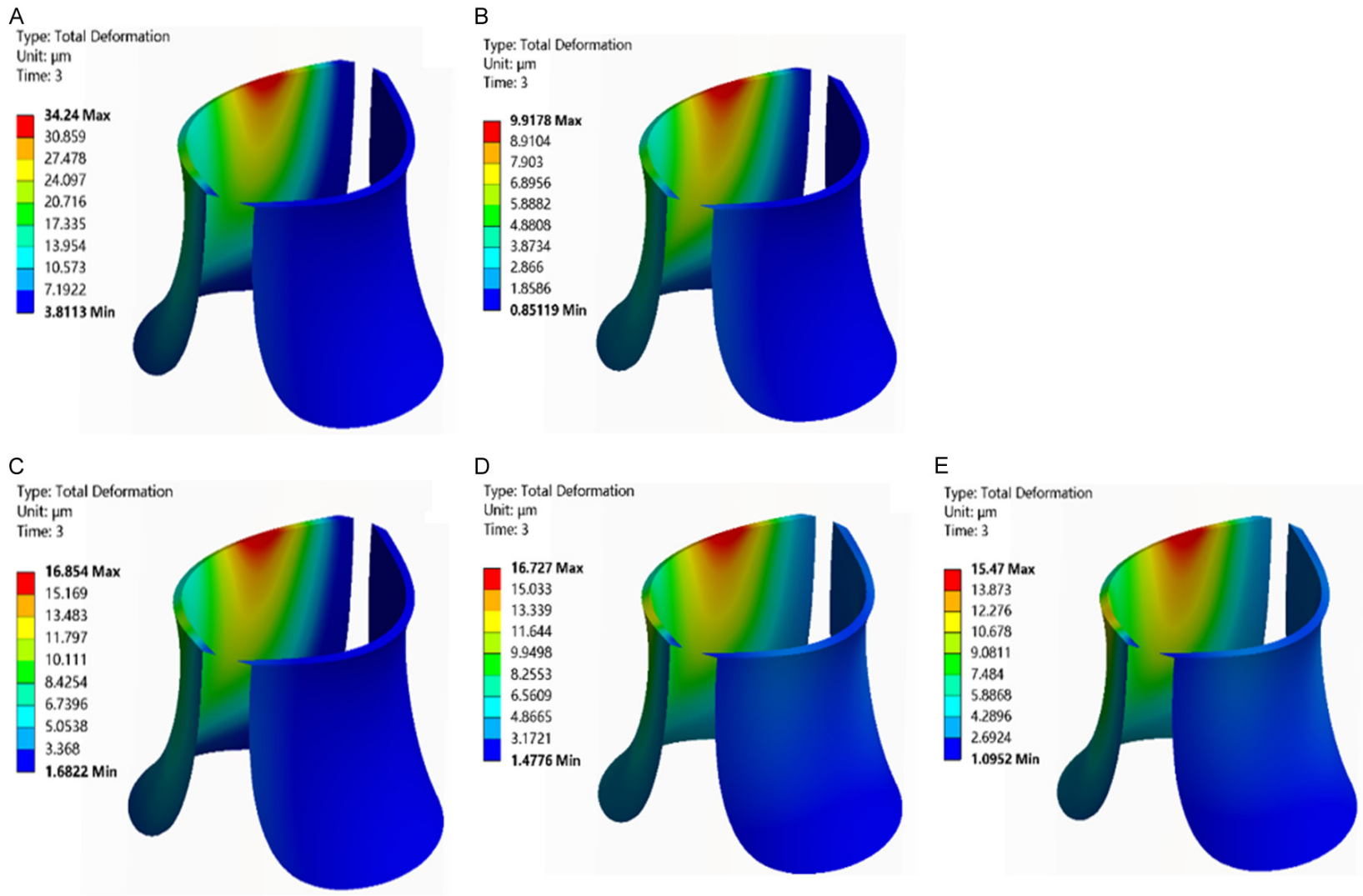

Figure 7. Total deformation of the venous valve. A. Normal group; B. HSS group; C. HT group; D. IPC group; E. IPCH group.

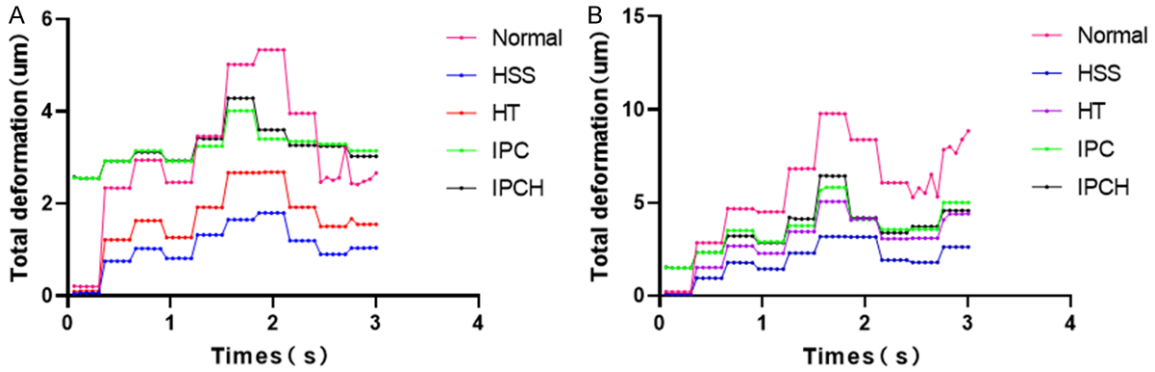

Figure 8. Relationship between total deformation and time. A. Femoral vein; B. Venous valve.

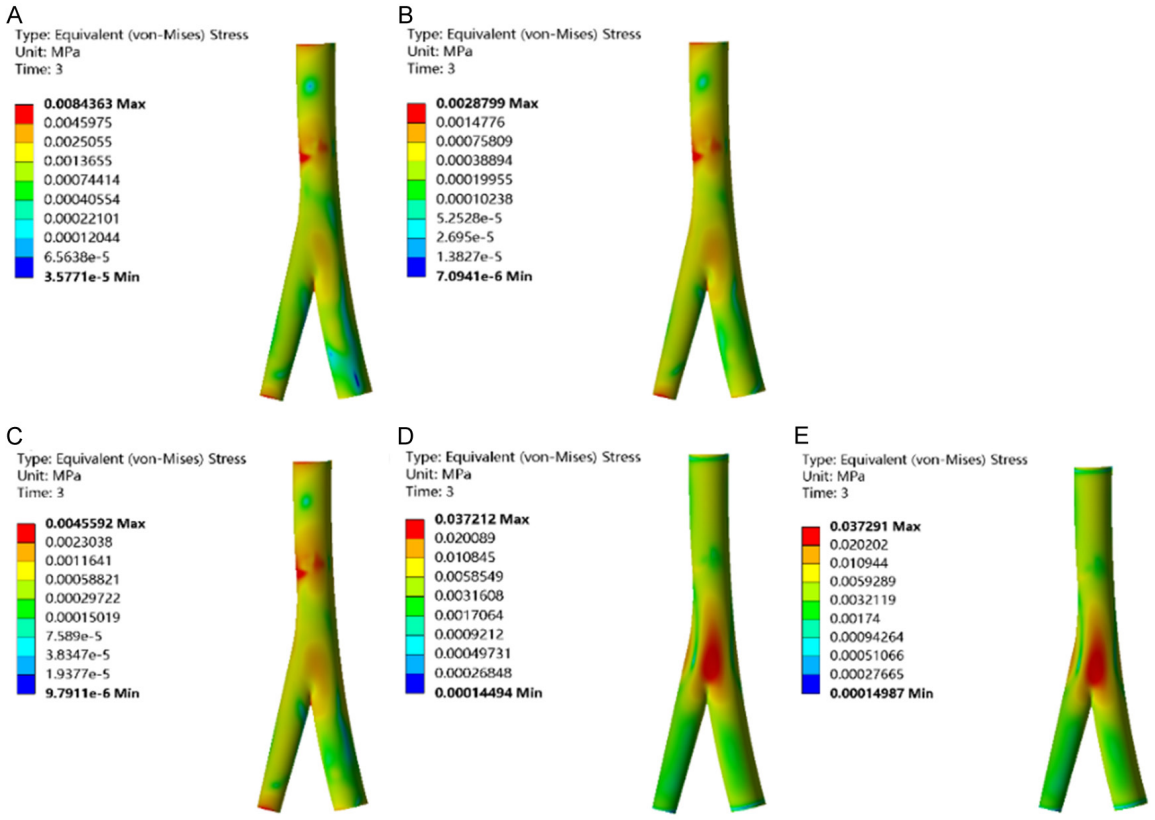

Figure 9. Equivalent stress of the femoral vein. A. Normal group; B. HSS group; C. HT group; D. IPC group; E. IPCH group.

stress of the femoral vein in the HT group was only slightly increased, but that in IPC and IPCH groups increased significantly, especially the equivalent stress at the saphenous-femoral junction. The IPCH group had the most significant increase, as shown in **Figure 9**.

Venous valve: In the Normal group, the equivalent stress of the left venous valve was significantly higher than that of the right venous valve, and the highest value was located at the rear of the left valve. The equivalent stress in the HSS group was significantly decreased, while that in HT, IPC, and IPCH groups increased to different degrees. The IPCH group showed the most significant increase, but the equivalent stress in the IPCH group was still lower than that of the Normal group, as shown in **Figure 10**.

Relationship between the change of equivalent stress and time: With the blood flowing from

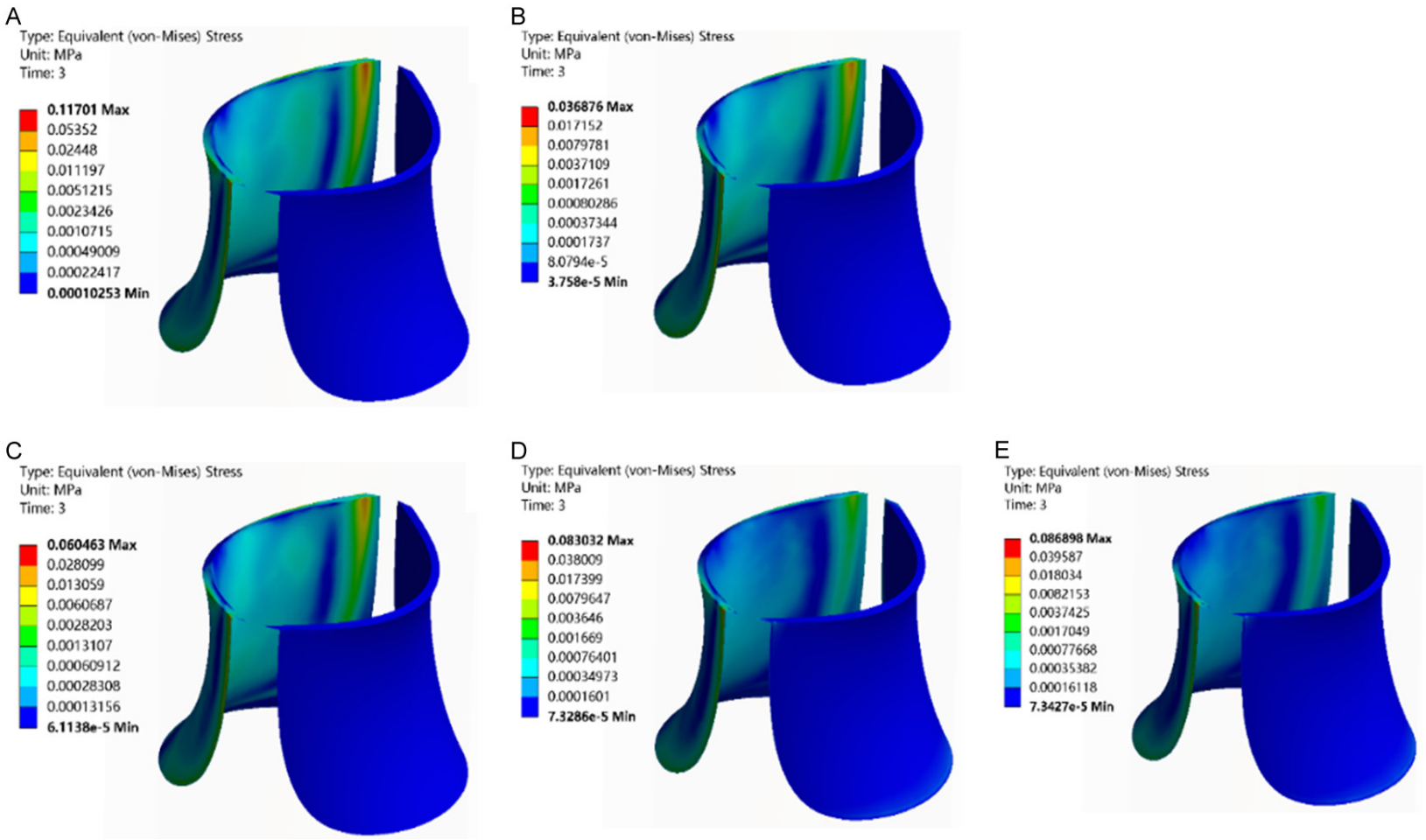

Figure 10. Equivalent stress of the venous valve. A. Normal group; B. HSS group; C. HT group; D. IPC group; E. IPCH group.

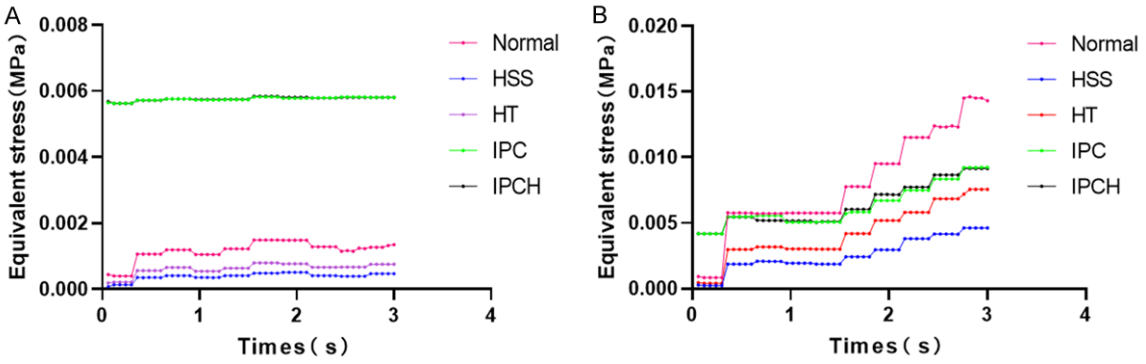

Figure 11. Relationship between the change of equivalent stress and time. A. Femoral vein; B. Venous valve.

the inlet, the equivalent stress of the femoral vein and venous valve gradually increased, and the most significant increase was in the venous valve. However, due to the pressure, the equivalent stress of the femoral vein increased significantly in IPC and IPCH groups, and was still higher than that of the Normal group. The equivalent stress of the venous valve increased continuously from 1.56 s after blood inflow. The equivalent stress of the venous valve in HT, IPC and IPCH groups was higher than that of the HSS group. The change in IPC and IPCH groups was more significant, but the equivalent stress of the venous valve in these two groups did not exceed that of the Normal group, as shown in **Figure 11**.

Discussion

The main finding of our study was that the actual efficacy of IPCH was significantly superior to the effect of application of IPC or HT alone. The IPCH group had a higher blood flow rate, and heart rate than the HT and IPC groups. The total deformation of the venous valve was relatively lower in the IPCH group. In addition, the blood velocity distribution, femoral venous total deformation, and equivalent stress of the femoral vein and venous valve in the IPCH group were higher than those in HT and IPC groups.

The physiologic mechanism of IPC to prevent DVT mainly includes mechanical and biochemical effects [30]. Calf "muscle pump" can significantly improve the volume, flow and velocity of blood vessels, and greatly promote venous blood backflow to the heart [31]. The mechanical effect of IPC is similar to the function of a "muscle pump": to conduct repeated sequential inflation and deflation of the multi-cavity air bag. The sequential step pressure of the air bag contributes to muscle contraction, to promote the blood in compressed deep veins of the lower limbs to flow back to the proximal vein during inflation, and flow to the distal vein during deflation. In this way, the deep veins of lower limbs can be periodically emptied, thus accelerating blood circulation of lower limbs to prevent DVT [32]. The biochemical effect of IPC is mainly achieved through increasing the shear and compression strain on endothelial cells by aerodynamic compression. Subsequently, the release of tissue-type plasminogen activator (t-PA), nitric oxide (NO), tissue factor pathway inhibitor and other bioactive mediators will occur, and expression of t-PA and endothelial NO synthase will be up-regulated, thereby activating the fibrinolysis system and promoting fibrinolysis in blood. The release of NO can also directly dilate blood vessels and inhibit the release of endothelin [33, 34]. Moreover, the application of IPC can inhibit the adhesion and aggregation of blood clotting factors to the intima of blood vessels to prevent DVT [35]. Thermal stimulation induces significant hemodynamic changes and metabolic regulation when applied to local tissues [36]. The increase of temperature can significantly reduce oxidative stress, improve NO bioavailability and vascular endothelial growth factor up-regulation, and ultimately improve the activity of vascular endothelial cells and promote vascular dilation of muscles and skin. In this way, blood perfusion will be effectively increased and blood circulation will be improved [20, 37, 38]. Thermal stimulation also induces the release of adenosine triphosphate (ATP), and increases myofibrin activity ATPase activity, and Ca^{2+} sensitivity, thereby promoting muscle contraction and improving blood circulation [39, 40].

By analyzing the hemodynamic parameters obtained by ultrasonic detection, it was found that the increase of peak blood velocity, mean blood velocity, and blood flow per minute in the IPCH group were significantly higher than those of HT and IPC groups. The results showed that the combined effect of IPC and HT could significantly change blood circulation in local lower limbs and even systemic blood circulation in rabbits. As a result of the improvement in blood circulation, the heart rate of rabbits increased to a certain extent. However, the diameter of the vessel did not change significantly, which may be related to the type of experimental animals. The veins of rabbits were relatively small, with an average diameter of 2.0±0.6 mm [41], and the scope of vascular dilatation was limited even under strong stimulation.

The venous valves are mostly open during the equilibrium phase. At this point, the blood flow diverged at the tip of the valve. Since the lumen formed by the tip of the valves is about 35% smaller than the distal vein, the blood flow velocity increased significantly in the narrow middle region when the venous valve was opened, which produced a jet. The main stream of venous blood flow was formed. The remaining blood flow (a small proportion) was channeled into the sinus cavity behind the valve tip, creating a vortex along the walls of the sinus and valve tip, and then flowed back into the main stream of the vein [42-44]. The blood velocity distribution in the three groups increased significantly; and the IPCH group had a more significant increase than the HT and IPC groups, which was consistent with the results of previous animal experiments. It was demonstrated that the effect of IPCH was better than that of a single application of IPC or HT. When we observed the blood velocity distribution, we also found vortexes in the area around the venous valve, where the velocity was significantly lower than that in other areas of the vein. Our preliminary study found that there was no direct correlation between the change of blood velocity and the vortex. This needs to be further verified by quantitative analysis.

IPC caused the deformation of vessels through intermittent progressive pressure. The femoral vein of rabbits was shallow, and the diameter was the largest at the saphenous-femoral junction. Therefore, the deformation of IPC and IPCH groups was most obvious at the saphenous-femoral junction. HT promoted vascular dilatation with an increase of temperature [45]. The femoral vein was deformed under the combined effect of intermittent pressure and temperature in the IPCH group, while it was deformed under single action of intermittent pressure or temperature in the IPC group and HT group. Therefore, the deformation of the femoral vein in the IPC and HT groups was not as obvious as that in the IPCH group. However, the deformation of the venous valve in the IPCH group was significantly less than that of the HT group. A possible reason was that IPCH activated and released some vasoactive substances, which led to a more apparent expansion of the venous lumen. Venous valve relative insufficiency already existed before venous valve was opened, and therefore the deformation was relatively small when the venous valve was opened.

According to the von Mises yield criterion, under certain deformation conditions, when the elastic deformation in the unit volume shape of the material changes to a certain constant, the material yields [46]. When the equivalent stress in a certain part of the vessel wall exceeds a constant, the risk of damage and rupture will increase, but IPC can produce mechanical and biochemical effects to improve blood circulation through intermittent compression [11, 47, 48]. In this study, the equivalent stress produced by IPCH was higher than that of the physiological state. The “physiological state” was a simulated relaxation status in which the blood vessels were not pressurized by muscles. However, in the human body, the lower limb blood vessels are squeezed by the contraction of the “muscle pump”, leading to equivalent stress. Moreover, the effect of this force on blood vessels is transient; that is, the effect occurs during “muscle pump” contractions and disappears during relaxation. Thus even if IPCH applied the equivalent stress repeatedly on the blood vessel wall, it only simulated the “muscle pump” and could not damage the blood vessel wall.

Taking this a step further, we believe that IPCH is closer to the physiologic state of muscle contraction, because the muscle during active contraction will produce heat [49, 50]. That is to say, in addition to muscle contraction, the release of ATP can also generate heat to speed up the local blood circulation. Moreover, heat is

also generated when Ca^{2+} binds to troponin C and parvalbumin at the beginning of contraction [51].

This study preliminarily explored the efficacy of IPCH, and whether it was superior to the effect of the single application of IPC or HT It lays the foundation for further investigations. However, this study has some limitations. First of all, male rabbits were selected as experimental animals. Although the effects of estrogen on the blood system were avoided, the lower limb anatomy of rabbits was quite different from the human body, which results in partial loss of compression effect caused by IPC. Secondly, the number of experimental animals was relatively small, and the weight was limited, so the femoral venous diameter did not change much in each group, resulting in some bias. Thirdly, in the hemodynamic analysis, since the femoral venous size in rabbits was small, the data of the venous valve could not be obtained. Only the diameter and thickness observed under the previous electron microscope were used to simulate the model, which may lead to a certain distortion of the model and bias in the experimental results.

Conclusion

The comprehensive effect of IPCH is significantly superior to the effect of application of IPC or HT alone. Even though IPCH significantly increase the rate of venous blood flow, it is unlikely to damage the venous wall.

Disclosure of conflict of interest

None.

Address correspondence to: Dr. Kan Jiang, Department of Orthopedics, Sixth Affiliated Hospital of Xinjiang Medical University, 39 Wuxing Nan Rd, Tianshan District, Urumqi 830002, Xinjiang, P. R. China. Tel: +86-13579810902; E-mail: jiangkanxy0225@163.com

References

[1] Markatos K, Savvidou OD, Foteinou A, Kosmadaki S, Trikoupis I, Goumenos SD and Papagelopoulos PJ. Hallmarks in the history and development of total hip arthroplasty. Surg Innov 2020; 27: 691-694.

[2] Taheriazam A, Saeidinia A and Keihanian F. Total hip arthroplasty and cardiovascular complications: a review. Ther Clin Risk Manag 2018; 14: 685-690.

[3] Lieberman JR and Heckmann N. Venous thromboembolism prophylaxis in total hip arthroplasty and total knee arthroplasty patients: from guidelines to practice. J Am Acad Orthop Surg 2017; 25: 789-798.

[4] Elbuluk AM, Kim KY, Chen KK, Anoushiravani AA, Schwarzkopf R and Iorio R. Respiratory synchronized versus intermittent pneumatic compression in prevention of venous thromboembolism after total joint arthroplasty: a systematic review and meta-analysis. Orthop Clin North Am 2018; 49: 123-133.

[5] Ruskin KJ. Deep vein thrombosis and venous thromboembolism in trauma. Curr Opin Anaesthesiol 2018; 31: 215-218.

[6] Stubbs MJ, Mouyis M and Thomas M. Deep vein thrombosis. BMJ 2018; 360: k351.

[7] Wang D, Bao F, Li Q, Teng Y and Li J. Semiautomatic intermittent pneumatic compression device applied to deep vein thrombosis in major orthopedic surgery. Biomed Eng Online 2018; 17: 78.

[8] Zhang ZH, Shen B, Yang J, Zhou ZK, Kang PD and Pei FX. Risk factors for venous thromboembolism of total hip arthroplasty and total knee arthroplasty: a systematic review of evidences in ten years. BMC Musculoskelet Disord 2015; 16: 24.

[9] Geerts WH, Pineo GF, Heit JA, Bergqvist D, Lassen MR, Colwell CW and Ray JG. Prevention of venous thromboembolism: the Seventh ACCP Conference on Antithrombotic and Thrombolytic Therapy. Chest 2004; 126 Suppl: 338S-400S.

[10] Dunn N and Ramos R. Preventing venous thromboembolism: the role of nursing with intermittent pneumatic compression. Am J Crit Care 2017; 26: 164-167.

[11] Morris RJ and Roberts CH. Haematological effects of intermittent pneumatic compression for deep vein thrombosis prophylaxis. Thromb Haemost 2020; 120: 912-923.

[12] Cesarman-Maus G and Ruiz-Argüelles GJ. News in the indications of direct oral anticoagulants according to the American College of Chest Physicians 2016 Guidelines. Curr Drug Metab 2017; 18: 651-656.

[13] Malanga GA, Yan N and Stark J. Mechanisms and efficacy of heat and cold therapies for musculoskeletal injury. Postgrad Med 2015; 127: 57-65.

[14] Wyper DJ and McNiven DR. The effect of microwave therapy upon muscle blood flow in man. Br J Sports Med 1976; 10: 19-21.

[15] Chiesa ST, Trangmar SJ and González-Alonso J. Temperature and blood flow distribution in the

human leg during passive heat stress. J Appl Physiol (1985) 2016; 120: 1047-58.
[16] Chiesa ST, Trangmar SJ, Kalsi KK, Rakobowchuk M, Banker DS, Lotlikar MD, Ali L and González-Alonso J. Local temperature-sensitive mechanisms are important mediators of limb tissue hyperemia in the heat-stressed human at rest and during small muscle mass exercise. Am J Physiol Heart Circ Physiol 2015; 309: H369-80.
[17] Rostrup E, Christensen MH, Seifert R and Nordrehaug JE. Physiological effects of combined thermal and electrical muscle stimulation (cTEMS) in healthy individuals: a pilot study. Scand J Clin Lab Invest 2012; 72: 237-45.
[18] Shen C, Li N, Chen B, Wu J, Wu Z, Hua D, Wang L, Chen D, Shao Z, Ren C and Xu J. Thermotherapy for knee osteoarthritis: a protocol for systematic review. Medicine (Baltimore) 2021; 100: e25873.
[19] Giombini A, Giovannini V, Di Cesare A, Pacetti P, Ichinoseki-Sekine N, Shiraishi M, Naito H and Maffulli N. Hyperthermia induced by microwave diathermy in the management of muscle and tendon injuries. Br Med Bull 2007; 83: 379-96.
[20] Inoue S, Takemoto M, Chishaki A, Ide T, Nishizaka M, Miyazono M, Sawatari H and Sunagawa K. Leg heating using far infra-red radiation in patients with chronic heart failure acutely improves the hemodynamics, vascular endothelial function, and oxidative stress. Intern Med 2012; 51: 2263-70.
[21] Sinclair ME, Simpson P, Marshall FP and Lockyer JA. Effect of varying methods of upper limb occlusion on fibrinolytic activity in man. Br J Anaesth 1984; 56: 175-7.
[22] Kiudelis M, Gerbutavicius R, Gerbutaviciene R, Griniūte R, Mickevicius A, Endzinas Z and Pundzius J. A combinative effect of low-molecular-weight heparin and intermittent pneumatic compression device for thrombosis prevention during laparoscopic fundoplication. Medicina (Kaunas) 2010; 46: 18-23.
[23] Hayashi K, Mori K and Miyazaki H. Biomechanical response of femoral vein to chronic elevation of blood pressure in rabbits. Am J Physiol Heart Circ Physiol 2003; 284: H511-8.
[24] Mühlberger D, Morandini L and Brenner E. An anatomical study of femoral vein valves near the saphenofemoral junction. J Vasc Surg 2008; 48: 994-9.
[25] Buss H, Schneider J and Hollweg HG. The endothelial surface of large veins of rabbit: scanning electron microscopic observations. Pathol Res Pract 1979; 165: 392-410.
[26] Lurie F and Kistner RL. The relative position of paired valves at venous junctions suggests their role in modulating three-dimensional flow pattern in veins. Eur J Vasc Endovasc Surg 2012; 44: 337-40.
[27] Soifer E, Weiss D, Marom G and Einav S. The effect of pathologic venous valve on neighboring valves: fluid-structure interactions modeling. Med Biol Eng Comput 2017; 55: 991-999.
[28] Shahcheraghi N, Dwyer HA, Cheer AY, Barakat AI and Rutaganira T. Unsteady and three-dimensional simulation of blood flow in the human aortic arch. J Biomech Eng 2002; 124: 378-87.
[29] Tien WH, Chen HY, Berwick ZC, Krieger J, Chambers S, Dabiri D and Kassab GS. Characterization of a bioprosthetic bicuspid venous valve hemodynamics: implications for mechanism of valve dynamics. Eur J Vasc Endovasc Surg 2014; 48: 459-64.
[30] Chen AH, Frangos SG, Kilaru S and Sumpio BE. Intermittent pneumatic compression devices -- physiological mechanisms of action. Eur J Vasc Endovasc Surg 2001; 21: 383-92.
[31] Hu X, Li Y, Li J and Chen H. Effects of altered blood flow induced by the muscle pump on thrombosis in a microfluidic venous valve model. Lab Chip 2020; 20: 2473-2481.
[32] Pavon JM, Adam SS, Razouki ZA, McDuffie JR, Lachiewicz PF, Kosinski AS, Beadles CA, Ortel TL, Nagi A and Williams JW Jr. Effectiveness of intermittent pneumatic compression devices for venous thromboembolism prophylaxis in high-risk surgical patients: a systematic review. J Arthroplasty 2016; 31: 524-32.
[33] Dai G, Tsukurov O, Chen M, Gertler JP and Kamm RD. Endothelial nitric oxide production during in vitro simulation of external limb compression. Am J Physiol Heart Circ Physiol 2002; 282: H2066-75.
[34] Rifkind JM, Nagababu E, Dobrosielski DA, Salgado MT, Lima M, Ouyang P and Silber HA. The effect of intermittent pneumatic compression of legs on the levels of nitric oxide related species in blood and on arterial function in the arm. Nitric Oxide 2014; 40: 117-22.
[35] Kohro S, Yamakage M, Sato K, Sato JI and Namiki A. Intermittent pneumatic foot compression can activate blood fibrinolysis without changes in blood coagulability and platelet activation. Acta Anaesthesiol Scand 2005; 49: 660-4.
[36] Kim K, Monroe JC, Gavin TP and Roseguini BT. Skeletal muscle adaptations to heat therapy. J Appl Physiol (1985) 2020; 128: 1635-1642.
[37] Kumaran B and Watson T. Thermophysiological responses to capacitive resistive monopolar radiofrequency electromagnetic radiation in patients with osteoarthritis of the knee joint: a randomised controlled experimental study. Electromagn Biol Med 2021; 40: 210-221.

[38] Pearson J, Low DA, Stöhr E, Kalsi K, Ali L, Barker H and González-Alonso J. Hemodynamic responses to heat stress in the resting and exercising human leg: insight into the effect of temperature on skeletal muscle blood flow. Am J Physiol Regul Integr Comp Physiol 2011; 300: R663-73.

[39] Ishii S, Oyama K, Shintani SA, Kobirumaki-Shimozawa F, Ishiwata S and Fukuda N. Thermal activation of thin filaments in striated muscle. Front Physiol 2020; 11: 278.

[40] Périard JD, Eijsvogels T and Daanen H. Exercise under heat stress: thermoregulation, hydration, performance implications, and mitigation strategies. Physiol Rev 2021; 101: 1873-1979.

[41] Barnat N, Grisey A, Lecuelle B, Anquez J, Gerold B, Yon S and Aubry JF. Noninvasive vascular occlusion with HIFU for venous insufficiency treatment: preclinical feasibility experience in rabbits. Phys Med Biol 2019; 64: 025003.

[42] Meissner MH, Moneta G, Burnand K, Gloviczki P, Lohr JM, Lurie F, Mattos MA, McLafferty RB, Mozes G, Rutherford RB, Padberg F and Sumner DS. The hemodynamics and diagnosis of venous disease. J Vasc Surg 2007; 46 Suppl S: 4S-24S.

[43] Lurie F, Kistner RL, Eklof B and Kessler D. Mechanism of venous valve closure and role of the valve in circulation: a new concept. J Vasc Surg 2003; 38: 955-61.

[44] Lurie F, Kistner RL and Eklof B. The mechanism of venous valve closure in normal physiologic conditions. J Vasc Surg 2002; 35: 713-7.

[45] Petrofsky J, Laymon M and Lee H. Local heating of trigger points reduces neck and plantar fascia pain. J Back Musculoskelet Rehabil 2020; 33: 21-28.

[46] Schwiedrzik JJ, Wolfram U and Zysset PK. A generalized anisotropic quadric yield criterion and its application to bone tissue at multiple length scales. Biomech Model Mechanobiol 2013; 12: 1155-68.

[47] Trinity JD and Richardson RS. Physiological impact and clinical relevance of passive exercise/movement. Sports Med 2019; 49: 1365-1381.

[48] Welsh JD, Hoofnagle MH, Bamezai S, Oxendine M, Lim L, Hall JD, Yang J, Schultz S, Engel JD, Kume T, Oliver G, Jimenez JM and Kahn ML. Hemodynamic regulation of perivalvular endothelial gene expression prevents deep venous thrombosis. J Clin Invest 2019; 129: 5489-5500.

[49] Barclay CJ and Loiselle DS. Historical perspective: heat production and chemical change in muscle. Roger C. Woledge. Prog Biophys Mol Biol 2021; 161: 3-16.

[50] Loiselle DS, Johnston CM, Han JC, Nielsen PM and Taberner AJ. Muscle heat: a window into the thermodynamics of a molecular machine. Am J Physiol Heart Circ Physiol 2016; 310: H311-25.

[51] Barclay CJ. Energetics of contraction. Compr Physiol 2015; 5: 961-95.